3D-QSAR Comparative Molecular Field Analysis on Opioid Receptor Antagonists: Pooling Data from Different Studies

Youyi Peng, Susan M. Keenan, Qiang Zhang, Vladyslav Kholodovych, and William J. Welsh*

Department of Pharmacology and the Informatics Institute of UMDNJ, University of Medicine & Dentistry of New Jersey−Robert Wood Johnson Medical School (UMDNJ−RWJMS), Piscataway, New Jersey 08854

Received November 3, 2004

Three-dimensional quantitative structure−activity relationship (3D-QSAR) models were constructed using comparative molecular field analysis (CoMFA) on a series of opioid receptor antagonists. To obtain statistically significant and robust CoMFA models, a sizable data set of naltrindole and naltrexone analogues was assembled by pooling biological and structural data from independent studies. A process of "leave one data set out", similar to the traditional "leave one out" cross-validation procedure employed in partial least squares (PLS) analysis, was utilized to study the feasibility of pooling data in the present case. These studies indicate that our approach yields statistically significant and highly predictive CoMFA models from the pooled data set of δ, μ, and κ opioid receptor antagonists. All models showed excellent internal predictability and self-consistency: $q^2 = 0.69/r^2 = 0.91$ (δ), $q^2 = 0.67/r^2 = 0.92$ (μ), and $q^2 = 0.60/r^2 = 0.96$ (κ). The CoMFA models were further validated using two separate test sets: one test set was selected randomly from the pooled data set, while the other test set was retrieved from other published sources. The overall excellent agreement between CoMFA-predicted and experimental binding affinities for a structurally diverse array of ligands across all three opioid receptor subtypes gives testimony to the superb predictive power of these models. CoMFA field analysis demonstrated that the variations in binding affinity of opioid antagonists are dominated by steric rather than electrostatic interactions with the three opioid receptor binding sites. The CoMFA steric−electrostatic contour maps corresponding to the δ, μ, and κ opioid receptor subtypes reflected the characteristic similarities and differences in the familiar "message−address" concept of opioid receptor ligands. Structural modifications to increase selectivity for the δ over μ and κ opioid receptors have been predicted on the basis of the CoMFA contour maps. The structure−activity relationships (SARs) together with the CoMFA models should find utility for the rational design of subtype-selective opioid receptor antagonists.

Introduction

Opioid receptors belong to the rhodopsin-like subfamily within the superfamily of G-protein coupled receptors (GPCRs).[1] Three opioid receptor subtypes, designated δ, μ, and κ, have been identified in the central nervous system (CNS) and periphery.[2,3] While the crystal structures of the opioid receptors remain unavailable, there is abundant biological and structural information for known ligands. Antagonists selective for the δ receptor modulate the development of tolerance and dependence induced by μ agonists such as morphine.[4] They also alter the behavioral effects of drugs of abuse, such as cocaine,[5] and evoke favorable immunomodulatory effects.[6] Furthermore, recent studies demonstrate that δ antagonists, when delivered in concert with μ agonists, result in effective pain modulation without the negative side effects (such as physical addiction) usually associated with μ receptor activation.[7]

Naltrindole (NTI, Figure 1), a nonpeptidic δ antagonist with high binding affinity ($K_i = 0.22$ nM) and moderate selectivity (selectivity ratio: $\mu/\delta = 120$, $\kappa/\delta = 138$) for the δ opioid receptor,[8] is widely used for the pharmacological characterization of opioid receptor subtypes. Recognition of NTI by the opioid receptors is attributed to the existence of the tyramine group, which fulfills the "message" component of the "message−address" system postulated for opioid ligands with morphine-like structures (Figure 1).[9] The high potency and selectivity for the δ receptor have been attributed to the conformationally constrained benzene moiety, which mimics the side chain of the putative "address" component (Phe[4]) of enkephalin.[9] Since the discovery of NTI by Portoghese et al.,[10] numerous NTI analogues have been synthesized and biologically evaluated to explore the structure−activity relationship (SAR) and to design more selective δ antagonists.[11−18]

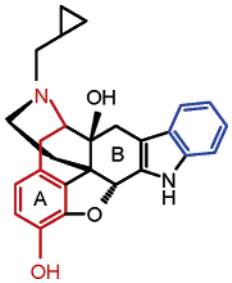

Figure 1. The structure of NTI. The "message" and "address" for δ opioid receptor are respectively colored in red and blue.

Molecular modeling techniques are valuable tools for drug design and can be used to rationalize the interaction of ligands with their target receptors. Three-

* To whom correspondence should be addressed. Tel: 732-235-3234. Fax: 732-235-3475. E-mail:welshwj@umdnj.edu.

10.1021/jm049117e CCC: $30.25
Published on Web 02/09/2005

dimensional quantitative structure−activity relationship (3D-QSAR) models, constructed by employing comparative molecular field analysis (CoMFA), are particularly effective in cases when the receptor structure is unknown. CoMFA samples the steric and electrostatic fields surrounding a set of ligands and constructs a 3D-QSAR model by correlating these 3D fields with the corresponding experimental activities of ligands with respect to a common target receptor.

The quality of the biological data set is paramount in building valid QSAR models. The range and distribution of the data set should meet certain requirements. Furthermore, biological data are prone to variation between laboratories and even between studies within the same laboratory. Such variations can confound attempts to model and interpret the biological data using QSAR and other molecular modeling techniques. As a consequence, mixing biological data retrieved from different laboratories or even from separate publications in the same laboratory is considered risky and is ordinarily discouraged. Nevertheless, pooling may be permissible in cases where a single source of plentiful high-quality data is lacking and when measures are taken to validate the resulting models. The present case study pertaining to opioid receptor ligands is a salient example.

In the present study, a large data set of opioid receptor antagonists with common pharmacophoric features was amalgamated from seven independently published data sources. The suitability of pooling data in this manner was explored using a "leave one data set out" cross-validation methodology. Statistically significant and highly predictive CoMFA models for all three receptor subtypes were obtained from the final pooled data set. Furthermore, these models predicted the biological activities of a structurally diverse array of compounds retrieved from additional published sources. By virtue of their unique ability to differentiate the structural requirements for ligand binding to the opioid receptor subtypes, these models offer utility in guiding the rational design of potent and selective δ opioid antagonists for therapeutic applications.

Experimental Section

All molecular modeling operations were performed on Silicon Graphics, Inc. (SGI) workstations. The crystal structure of Naltrexone[19] was used as the starting conformation for subsequent construction of NTI and its analogues. The structures were built with the Sybyl 6.8 molecular modeling software package.[20] The MMFF94 force field and partial atomic charges were used to optimize the geometries of all compounds. All compounds were protonated at atom N17 (Table 1) in the same spatial location.

Data Collection. Data from seven separately published articles using identical binding assay protocols[8,11−16] were combined for our CoMFA studies. Briefly, the competitive binding assays were performed against rat brain membrane for δ and μ receptors and guinea pig brain membrane for the κ receptor. The competitive ligands for the δ, μ, and κ receptors were [^{3}H]DADLE, [^{3}H]DAMGO, and [^{3}H]U69593, respectively. A total of 74 compounds with detectable binding affinity for the δ receptor were pooled, yielding a data set that spanned >5 logarithmic (log) units in terms of pK_i and contained seven distinct core structures (Table 1). The experimental biological activities of the data set compounds are evenly distributed: 16 weakly active compounds (pK_i < 7.0), 30 moderately active compounds (7.0 < pK_i < 8.0), and 29 highly active compounds (pK_i > 8.0).

As is customary for CoMFA, the data set was separated into a training set (61 compounds) for final model development and a test set (13 compounds) for model validation. The test-set compounds were chosen randomly with some bias toward ensuring representation from the full range of biological data in the training set. The resulting test set contained 3 weakly active, 5 moderately active, and 5 highly active compounds.

To permit comparison among the separate models constructed for the three receptor subtypes, only compounds with δ binding affinity (i.e., compounds used to develop and validate the δ model) were considered for the μ and κ CoMFA models. Of the 58 (59) compounds also exhibiting binding affinity for the μ (κ) receptor, the training set consisted of 48 (49) compounds. The test sets in both cases consisted of 10 compounds: 7 weakly active, 2 moderately active, and 1 highly active compounds. The structures and measured binding affinities (pK_i) of all compounds are shown in Table 1.

To further evaluate the predictability of the CoMFA models, a diverse collection of 27 compounds from other published reports was selected as an external test set and predicted by the models.[21−24] The compounds with pyridomorphinan (**73**−**82**) and phenylmorphan (**97**−**100**) core structures were biologically evaluated by the same assay as the pooled compounds (i.e., δ and μ binding affinity on rat brain membrane; κ binding affinity on guinea pig brain membrane with the same radiolabeled competitive ligands). However, the compounds with cyprodime and NTI core structures (**83**−**96**) were tested on rat brain membrane for all three opioid receptors. The competitive ligands for the δ, μ, and κ receptors were [^{3}H][Ile^{5,6}]-deltorphin II, [^{3}H]DAMGO, and [^{3}H]U69593, respectively. The structures and binding affinities (pK_i) of these compounds are shown in Table 2. Aside from the phenylmorphan analogues, these compounds were aligned to NTI with the same alignment scheme as the pooled compounds. The phenylmorphan analogues were aligned to NTI by fitting the phenolic ring and the basic nitrogen atom.

CoMFA Procedure. NTI, the most active δ opioid receptor compound, was selected as the template for aligning the compounds in the training and test sets. Since all ligands are fairly rigid and share key pharmacophoric features, the *atom-fit* method was employed for ligand alignment. Specifically, three atoms were chosen for the alignment: the basic nitrogen N17 and the pseudoatoms at the centroids of rings A and B (Table 1). The standard CoMFA procedure as implemented in Sybyl 6.8 was performed. Each ligand was placed in a 3D lattice with grid points separated by 2 Å. A C_{sp^3} atom with a formal charge of +1 and a van der Waals radius of 1.52 Å served as the probe. The steric (van der Waals) and electrostatic (Coulombic) interactions were calculated at each grid point by summing the individual interaction energies between each atom of the ligand molecule and the probe atom. A distance-dependent dielectric function $\epsilon = \epsilon_0 R_{ij}$ with $\epsilon_0 = 1.0$ was adopted to apply Coulomb's law. The computed field energies were truncated to 30 kcal/mol for the steric fields and to ±30 kcal/mol for the electrostatic fields.

Partial Least-Squares Analysis. The partial least-squares (PLS) technique was employed to generate a linear relationship that correlates changes in the computed steric and electrostatic potential fields with changes in the corresponding experimental values of the binding affinity (pK_i) for the data set of ligands. Employing the CoMFA potential energy fields for each molecule as the independent variable and the corresponding pK_i values as the dependent variable, PLS converts the steric and electrostatic field descriptors to so-called latent variables or principal components (PCs) that consist of linear combinations of the original independent variables.

To assess the internal predictive ability of the CoMFA models, we employed both "leave one data set out" and "leave one out" cross-validation procedures. In this procedure, each data set or compound is excluded one at a time, after which its activity is predicted by the model constructed from the remaining compounds in the data set. Cross-validation determines the optimum number of PCs, corresponding to the smallest error of prediction and the highest cross-validated

Table 1. Opioid Receptor Antagonists Considered in the Present Study[a]

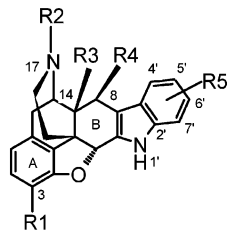

Core 1

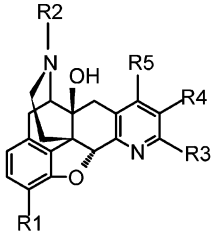

Core 2

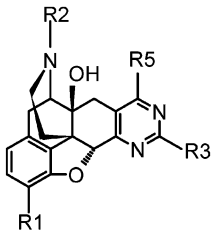

Core 3

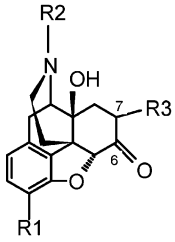

Core 4

Core 5

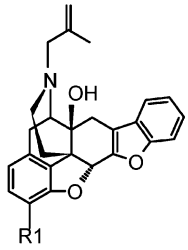

Core 6

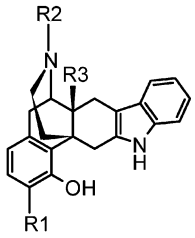

Core 7

							pK_i						
							exptl			pred			
compd	core	R1	R2	R3	R4	R5	δ	μ	κ	δ	μ	κ	ref
NTI	1	OH	CPM	OH	H	H	9.66	7.57	7.52	9.39	7.08	7.28	11
NTX	4	OH	CPM	H			7.40	8.60	8.15	7.87	8.73	8.47	13
1	1	OH	Et	OH	H	H	8.30	5.60	5.52	8.28	6.21	5.73	11
2	1	OH	n-Pr	OH	H	H	8.70	6.15	6.42	8.13	TS	6.45	11
3	1	OH	n-Bu	OH	H	H	8.08	5.89	6.05	7.99	5.59	5.85	11
4	1	OH	n-pentyl	OH	H	H	7.80	5.55	5.70	7.80	5.63	5.94	11
5	1	OH	n-hexyl	OH	H	H	7.59	5.34	5.51	7.63	5.53	TS	11
6	1	OH	n-heptyl	OH	H	H	7.10	5.34	–	TS	TS	–	11
7	1	OH	i-Pr	OH	H	H	7.48	–	5.21	7.90	–	5.55	11
8	1	OH	2-Me-Pr	OH	H	H	8.42	5.59	6.19	8.29	5.96	6.11	11
9	1	OH	3-Me-Bu	OH	H	H	8.42	5.89	6.17	8.12	5.78	TS	11
10	1	OH	*E*-cronyl	OH	H	H	8.13	5.92	6.02	8.04	5.87	6.04	11
11	1	OH	2-Me-allyl	OH	H	H	8.33	5.10	5.42	TS	5.67	5.58	11
12	1	OH	3-Me-cronyl	OH	H	H	7.60	5.55	5.49	7.80	5.55	5.80	11
13	1	OH	CPM	OH	H	4-Ph	7.28	5.82	5.53	TS	TS	5.36	12
14	1	OH	CPM	OH	H	4-OPh	7.17	5.84	5.88	7.55	6.05	TS	12
15	1	OH	CPM	OH	H	4-OBz	7.83	6.44	6.27	7.60	6.13	6.16	12
16	1	OH	CPM	OH	H	5-Ph	7.80	6.78	6.45	8.11	6.85	6.44	12
17	1	OH	CPM	OH	H	5-OPh	7.75	6.53	7.12	7.86	6.63	7.09	12
18	1	OH	CPM	OH	H	5-OBz	8.36	7.09	7.09	8.18	7.17	7.02	12
19	1	OH	CPM	OH	H	6-Ph	7.74	5.89	6.20	TS	5.81	6.21	12
20	1	OH	CPM	OH	H	6-OPh	8.19	6.63	6.63	7.87	6.56	6.62	12
21	1	OH	CPM	OH	H	6-OBz	8.17	6.17	6.33	8.16	5.92	6.44	12
22	1	OH	CPM	OH	H	7-Ph	8.68	6.91	6.51	8.66	6.58	6.38	12
23	1	OH	CPM	OH	H	7-OPh	9.15	7.47	7.47	8.67	7.33	TS	12
24	1	OH	CPM	OH	H	7-OBz	8.51	6.80	6.59	9.33	6.73	6.55	12
25	1	OH	CPM	OH	H	5-*E*-Py	8.43	7.12	7.70	8.10	TS	7.74	12
26	1	H	CPM	OH	H	H	7.46	–	4.96	8.18	–	5.02	16
27	1	Me	CPM	OH	H	H	7.15	–	–	TS	–		16
28	1	vinyl	CPM	OH	H	H	7.21	–	4.75	6.98	–	4.60	16
29	1	2-furanyl	CPM	OH	H	H	6.02	–	–	6.12	–	–	16
30	1	Ph	CPM	OH	H	H	4.98	–	–	5.38	–	–	16
31	1	3-OH-Ph	CPM	OH	H	H	5.79	–	–	5.38	–	–	16
32	1	OMe	Me	H	H	H	7.02	–	–	7.07	–	–	14
33	1	OMe	Me	H	Me	H	7.57	–	–	7.33	–	–	14
34	1	OMe	Me	H	n-Bu	H	6.43	–	–	6.10	–	–	14
35	1	OH	Me	H	H	H	8.62	6.15	–	8.36	6.49	–	14
36	1	OH	Me	H	Me	H	9.15	6.62	6.90	8.62	TS	TS	14
37	1	OH	Me	H	n-Bu	H	7.66	5.96	6.14	TS	6.47	5.93	14
38	1	OH	CPM	H	Me	H	8.64	7.18	7.44	9.20	6.77	7.24	14
39	1	OH	2-Me-allyl	H	Me	H	8.05	5.97	6.07	TS	5.61	6.08	14
40	1	OH	*E*-cronyl	H	Me	H	8.64	5.99	6.92	8.75	6.19	6.99	14
41	7	OMe	Me	H	–	–	7.03	5.55	–	7.26	5.45	–	8
42	7	OMe	Et	H	–	–	6.29	5.87	5.44	TS	5.55	5.29	8
43	7	OMe	CPM	H	–	–	8.15	4.88	5.10	7.90	5.28	TS	8
44	7	OMe	Me	OH	–	–	6.66	5.55	–	6.79	TS	–	8
45	7	OMe	Et	OH	–	–	6.16	6.10	–	6.48	5.86	–	8
46	7	OMe	CPM	OH	–	–	7.66	5.73	5.50	7.45	5.60	5.66	8
47	2	OH	CPM	H	H	H	9.11	8.82	8.06	TS	8.66	TS	13

Table 1 (Continued)

							pK_i						
							exptl			pred			
compd	core	R1	R2	R3	R4	R5	δ	μ	κ	δ	μ	κ	ref
48	2	OH	CPM	Ph	H	H	8.75	7.96	7.74	TS	8.12	7.72	13
49	2	OH	CPM	H	Ph	H	9.06	7.87	7.75	8.74	7.71	7.78	13
50	2	OH	CPM	H	4-Cl-Ph	H	8.66	7.29	7.70	8.51	7.58	7.59	13
51	2	OH	CPM	H	H	Ph	7.14	6.72	6.58	7.06	6.76	TS	13
52	2	OH	CPM	Me	H	Ph	6.90	6.81	6.17	TS	6.62	6.28	13
53	2	OH	CPM	Ph	H	Ph	7.07	6.19	5.67	6.85	6.23	5.77	13
54	2	OH	CPM	$(CH{=}CH)_2$		Ph	7.14	6.51	6.57	7.14	6.22	6.23	13
55	3	OH	CPM	H	–	H	8.46	8.38	8.20	8.13	TS	8.50	13
56	3	OH	CPM	Me	–	H	7.64	8.22	7.60	8.12	8.27	TS	13
57	3	OH	CPM	Ph	–	H	7.80	7.66	7.9 6	7.73	TS	7.79	13
58	3	OH	CPM	H	–	Ph	6.64	6.46	6.67	6.80	6.68	6.55	13
59	3	OH	CPM	Me	–	Ph	6.49	6.60	6.25	6.70	6.66	6.41	13
60	3	OH	CPM	Bz	–	Ph	7.00	6.63	5.90	6.93	6.49	5.92	13
61	3	OH	CPM	Ph	–	Ph	6.46	5.93	5.60	6.36	TS	5.84	13
62	1	OH	2-Me-allyl	OH	H	H	8.33	5.10	5.42	8.08	5.42	5.32	15
63	1	OMe	2-Me-allyl	OH	H	H	6.30	–	–	6.87	–	–	15
64	2	OH	2-Me-allyl	H	4-Cl-Ph	H	7.80	–	6.52	TS	–	6.42	15
65	2	OMe	2-Me-allyl	H	4-Cl-Ph	H	6.59	–	5.49	6.66	–	5.41	15
66	4	OH	2-Me-allyl	SI	–	–	7.39	5.70	6.00	7.48	5.41	6.06	15
67	4	OH	2-Me-allyl	=CHPh	–	–	6.68	5.35	5.35	6.70	5.40	5.28	15
68	4	OMe	2-Me-allyl	=CHPh	–	–	5.47	–	–	5.42	–	–	15
69	5	OH	–	–	–	–	7.40	6.85	7.42	7.40	TS	6.90	15
70	5	OMe	–	–	–	–	5.62	–	5.51	TS	–	5.85	15
71	6	OH	–	–	–	–	8.09	5.89	6.24	8.10	6.25	TS	15
72	6	OMe	–	–	–	–	7.36	–	–	7.36	–	–	15

[a] CPM, cyclopropylmethyl; Bz, benzyl; Py, pyridinyl; SI, spiroindanyl; 5′-*E*-Py, 5′-*E*-CH=CH-2-pyridinyl; TS, test set; –, no value available; p$K_i = -\log K_i$.

q^2 (or r^2_{cv}). PLS analysis was repeated without validation using the optimum number of PCs to generate a final CoMFA model from which the conventional r^2, a measure of the internal consistency of the model, was derived. To improve efficiency and reduce "noise", a column filter was applied by omitting from the analysis those columns (lattice points) with an energy variance <2.0 kcal/mol. All CoMFA models are represented as color contour maps to enable visualization of those steric and electrostatic fields that significantly contribute to a model.

Results and Discussion

Pooling Data from Independent Studies. To achieve a statistically significant 3D-QSAR model, certain criteria for data set parameters should be met. As a rule of thumb, the following conditions should be satisfied: (1) a minimum range of three log units for compound binding affinity, (2) no less than ~20 compounds (corresponding to approximately 5 compounds per PC) for model development, and (3) the biological activities of the compounds should be evenly distributed. Since within- and between-laboratory variations in pharmacological data are virtually unavoidable, all possible efforts should be taken to obtain the biological data from a single source. When this is not possible or feasible, as is the case with these opioid receptor antagonists, extra precautions should be taken to validate mixing of multisource data.

As delineation of the binding and receptor subtype specificity for opioid receptor activation has important clinical implications, we examined the possibility of pooling ligand binding data from separate published studies. One mandatory requirement for pooling such biological data is that they are derived using identical experimental protocols. We retrieved biological data from seven independent publications, each of which reported results for 6–15 NTI analogues using the same assay and radiolabeled competitive binding ligands (i.e., [^{3}H]DADLE (δ), [^{3}H]DAMGO (μ), and [^{3}H]U69593 (κ)). Taken alone, each individual data set is unable to fulfill the necessary requirements for model development. Collectively however, the combined data set of 74 compounds derived from seven core structures (Table 1) exhibits biological data that are evenly distributed over >5 log units in term of δ binding affinity (pK_i).

To examine the feasibility of utilizing these combined data, preliminary CoMFA studies were performed for all 74 compounds based on the binding affinity for the δ receptor subtype. A process of "leave one data set out", analogous to the standard "leave one out" cross-validation implemented in PLS analysis, was conducted in which ligands taken from each publication (e.g., set S1 in Table 3) were systematically excluded from the training data set and served as the test set for model validation. Standard PLS analyses were carried out for the remaining compounds (e.g., Model-S1). Each of these seven CoMFA models (Model-S1 to Model-S7) produced strong indicators of statistical significance ($r^2 > 0.85$) and internal predictive ability ($q^2 > 0.60$) using only four PCs (Table 3). All compounds in the test data sets were predicted well (i.e., <1 log unit of experimental pK_i) aside from a single set,[16] where the compounds exhibited notably lower pK_i values than the training-set compounds. On the basis of this preliminary analysis, we conclude that pooling data from different sources is a feasible strategy for CoMFA model development in the present case.

Development of the Final CoMFA Models. We selected 61, 48, and 49 compounds as the training sets to develop 3D-QSAR models for the δ, μ, and κ opioid receptor antagonists, respectively. The corresponding CoMFA-PLS models yielded excellent internal predictability and consistency with $q^2 = 0.69/r^2 = 0.91$, $q^2 = 0.67/r^2 = 0.92$, and $q^2 = 0.60/r^2 = 0.96$ (Table 4). The

Table 2. Molecular Structures and Binding Affinities of External Test-Set Compounds

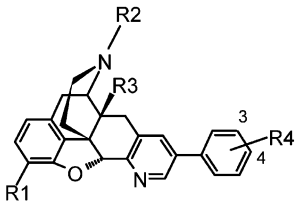

73-82

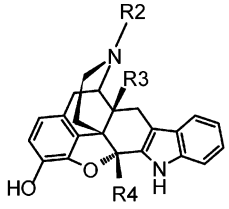

83-85

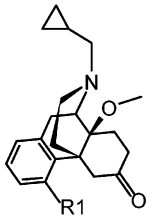

86-92

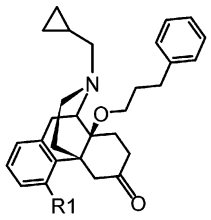

93-95

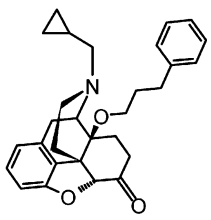

96

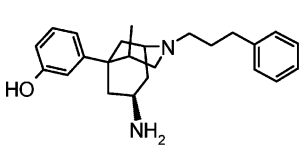

97

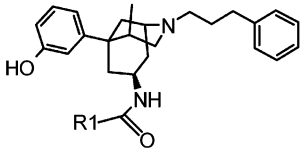

98-100

					pK_i									
					δ			μ			κ			
compd	R1	R2	R3	R4	exptl	pred	res[a]	exptl	pred	res[a]	exptl	pred	res[a]	ref
73	OH	allyl	OH	4-Cl	8.09	8.16	−0.07	6.33	7.01	−0.68	7.12	6.73	0.39	22
74	OH	Me	OH	H	8.54	8.11	0.43	7.59	7.61	−0.02	6.44	7.04	−0.60	22
75	OH	Me	OH	4-Cl	8.41	7.92	0.49	6.64	7.49	−0.85	6.33	6.86	−0.53	22
76	OH	Me	OH	4-Br	8.40	7.90	0.50	6.71	7.47	−0.76	6.36	6.82	−0.46	22
77	OH	Me	H	H	8.31	8.26	0.05	7.62	7.49	0.13	7.09	7.36	−0.27	22
78	OH	Me	H	4-Cl	8.36	8.06	0.30	6.83	7.40	−0.57	7.11	7.15	−0.04	22
79	OH	Me	H	4-Br	8.30	8.05	0.25	6.70	7.39	−0.69	7.04	7.18	−0.14	22
80	OH	Me	H	3,4-Cl	8.43	7.95	0.48	7.03	7.36	−0.33	6.56	6.95	−0.39	22
81	OH	Me	H	2,4-Cl	8.96	8.21	0.75	7.01	7.40	−0.39	6.39	7.12	−0.73	22
82	OH	CPM	H	4-Cl	8.59	8.67	−0.08	7.21	7.46	−0.25	8.22	7.84	0.38	22
83	−	CPM	OEt	Me	9.10	8.86	0.24	7.41	6.49	0.92	7.23	6.80	0.43	24
84	−	allyl	OEt	Me	7.97	8.49	−0.52	6.18	5.91	0.27	6.12	5.88	0.24	24
85	−	Me	OEt	Me	8.24	8.22	0.02	6.15	6.34	−0.19	6.54	5.9	0.64	24
87			OMe		6.38	7.35	−0.97	7.97	7.98	−0.01	6.96	7.47	−0.51	23
88			O(n-Bu)		6.12	7.09	−0.97	7.86	7.98	−0.12	6.58	7.40	−0.82	23
89			O(cinnamyl)		6.08	6.43	−0.35	7.55	8.07	−0.52	6.44	7.40	−0.96	23
90			$O(CH_2)_3Ph$		5.85	6.52	−0.67	7.36	8.00	−0.64	6.68	7.23	−0.55	23
91			OCH_2Ph		6.67	5.99	0.68	7.94	8.04	−0.10	7.25	6.84	0.41	23
92			O(n-hexyl)		5.93	6.39	−0.46	7.35	7.97	−0.62	6.36	7.28	−0.92	23
93			OH		8.30	7.50	0.80	9.40	8.10	1.30	8.23	7.38	0.85	23
94			OMe		7.77	7.36	0.41	9.47	7.81	1.66	8.13	7.33	0.80	23
95			O(n-Bu)		6.63	7.10	−0.47	7.83	7.88	−0.05	6.82	7.32	−0.50	23
96	−	−	−	−	7.34	7.41	−0.07	9.08	8.33	0.75	7.64	6.89	0.75	23
97	−	−	−	−	7.83	7.20	0.63	8.48	7.84	0.64	6.91	7.03	−0.12	21
98			$(CH_2)_3N(CH_3)_2$		5.84	6.57	−0.73	7.24	7.19	0.05	7.92	7.36	0.56	21
99			$(CH_2)_2NHC(=CH)NH_2$		7.25	7.45	−0.20	8.28	7.16	1.12	7.63	6.87	0.76	21
100			$(CH_2)_3NHC(=CH)NH_2$		5.76	6.41	−0.65	7.06	6.3	0.76	7.88	7.14	0.74	21

[a] The residual (res) corresponds to the signed difference between the experimental and CoMFA-predicted pK_i value.

strong correlation between observed and CoMFA-predicted pK_i values for all three opioid receptor subtypes is evident from the tabulated results (Table 1) and corresponding plots (parts A, B, and C of Figure 2, respectively).

The predictive power of the CoMFA models was validated for these δ, μ, and κ antagonists using the test sets. Selection of the test-set compounds was conducted randomly, except that some bias was applied to ensure adequate coverage in terms of binding affinity and structural variation. Comparison of the experimentally observed and CoMFA-predicted pK_i values of the δ, μ,

Table 3. Summary of Statistical Parameters for the Preliminary CoMFA Studies[a]

model	PC	q^2	SEE	r^2	F
S1	4	0.72	0.32	0.91	137
S2	4	0.62	0.31	0.89	122
S3	4	0.69	0.28	0.92	171
S4	4	0.75	0.34	0.89	115
S5	4	0.75	0.30	0.91	152
S6	4	0.71	0.31	0.91	129
S7	4	0.70	0.01	0.90	135

[a] SEE, standard error of estimate; F, F ratio, defined as $r^2/(1 - r^2)$ and representing the ratio of properties explained by the QSAR model to those not explained by it.[36]

Table 4. Summary of Results, Including Statistical Parameters, for Final CoMFA models of the δ, μ and κ Antagonists

	size of training set	size of test set	PCs	q^2	r^2	SEE	F	steric %	electrostatic %	predictive r^2
δ	61	13	4	0.69	0.91	0.29	146	75	25	0.70
μ	48	10	4	0.67	0.92	0.27	118	65	35	0.89
κ	49	10	6	0.60	0.96	0.19	162	67	33	0.77

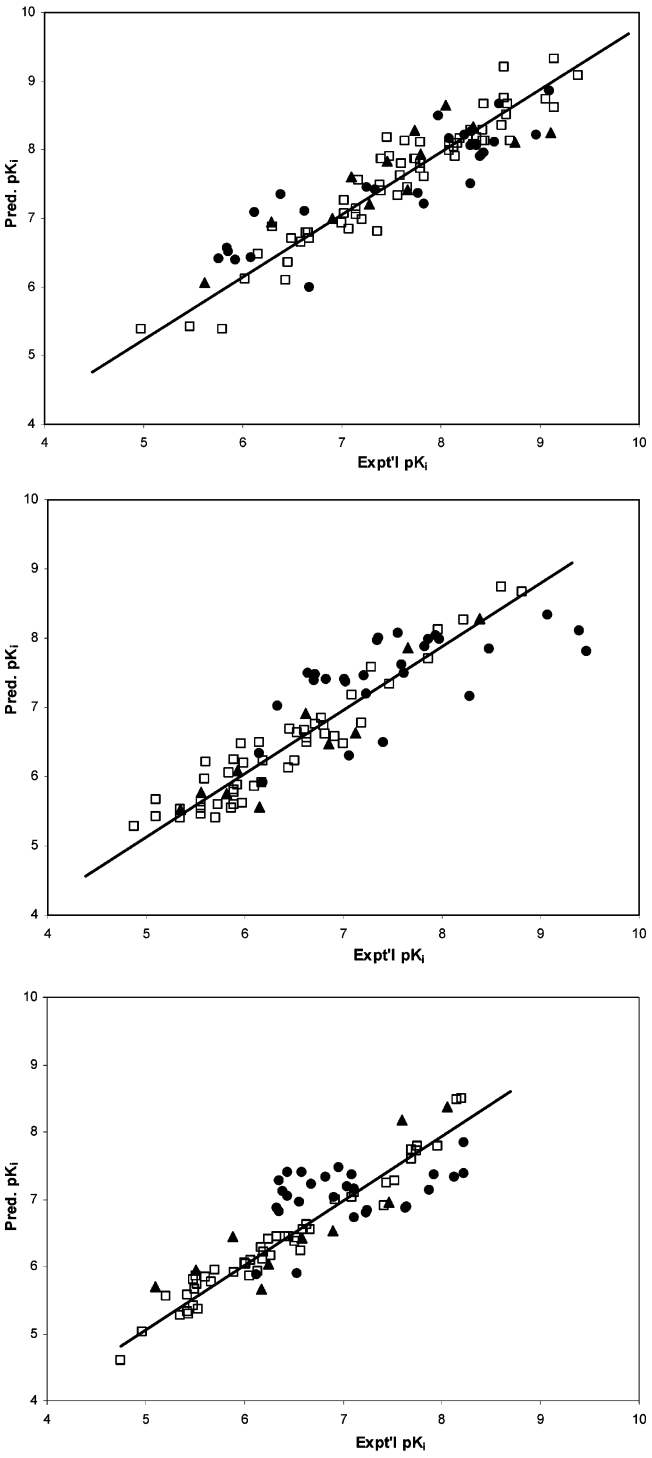

Figure 2. A plot of CoMFA-predicted vs experimental pK_i values of the training-set, test-set, and external test-set compounds for the δ (A: upper), μ (B: middle), and κ (C: lower) opioid receptors: (□) training set, (▲) test set, (●) external test set.

and κ antagonists in the respective test sets (Tables 5, 6, and 7; Figure 2, parts A, B, and C) further confirms the predictive ability of the models. The residuals

Table 5. Comparison of Experimental and Predicted pK_i Values of the Test-Set Compounds for the δ Antagonist CoMFA Model

	pK_i				pK_i		
compd	exptl	pred	res	compd	exptl	pred	res
6	7.10	7.63	−0.53	42	6.29	6.94	−0.55
11	8.33	8.33	0.00	47	9.11	8.24	0.87
13	7.28	7.18	0.10	48	8.75	8.11	0.64
19	7.74	8.28	−0.54	52	6.90	7.00	−0.10
27	7.46	7.83	−0.39	64	7.80	7.94	−0.14
37	7.66	7.41	0.25	70	5.62	6.09	−0.47
39	8.05	8.64	−0.59				

Table 6. Comparison of Experimental and Predicted pK_i Values of the Test-Set Compounds for the μ Antagonist CoMFA Model

	pK_i				pK_i		
compd	exptl	pred	res	compd	exptl	pred	res
2	6.15	5.57	0.58	44	5.55	5.78	−0.23
6	5.34	5.53	−0.19	55	8.38	8.28	0.10
13	5.82	5.75	0.07	57	7.66	7.86	−0.20
25	7.12	6.64	0.48	61	5.93	6.09	−0.16
36	6.62	6.92	−0.30	69	6.85	6.48	0.37

Table 7. Comparison of Experimental and Predicted pK_i Values of the Test-Set Compounds for the κ Antagonist CoMFA Model

	pK_i				pK_i		
compd	exptl	pred	res	compd	exptl	pred	res
5	5.51	5.94	−0.43	43	5.10	5.70	−0.60
9	6.17	5.67	0.50	47	8.06	8.37	−0.21
14	5.88	6.44	−0.58	51	6.58	6.42	0.16
23	7.47	6.95	0.52	56	7.60	8.18	−0.58
36	6.90	6.53	0.37	71	6.24	6.04	0.20

(differences) between corresponding values of the experimental and predicted binding affinity are <1 log unit, and all test-set compounds follow the regression trend line established by the training sets. In addition, the CoMFA-predicted pK_i values of the δ, μ, and κ test-set compounds gave high values of the predictive r^2, 0.70, 0.89, and 0.77, respectively (Table 4). Defined analogously to q^2, the predictive r^2 is used to evaluate the overall performance of a model by comparing the accuracy of a series of predictions with the experimentally known target property data. Successive application of "leave 10 out" cross-validation on the data set for 50, 100, and 150 times yielded consistent results with $q^2 > 0.60$ (data not shown). The exceptional statistical robustness of these CoMFA models adds confidence in their utility for predicting the binding affinity of NTI opioid-receptor antagonists. It also further corroborates the validity of pooled experimental data in the present case.

Validation of CoMFA Models by External Test-Set Compounds. Twenty-seven compounds, representing five distinct core structures (Table 2), were selected from other publications as an external test set to further evaluate the predictability of the CoMFA models. The

core structures in this external test set differ substantially in many cases from those included in the CoMFA models. It is noteworthy that none of the cyprodime and phenylmorphan analogues were included in the development of the present CoMFA models. Moreover, for these cyprodime analogues, the δ binding affinities were measured using a different competitive ligand (viz., [^{3}H]-[Ile^{5,6}]deltorphin II rather than [^{3}H]DADLE), and the κ binding affinities were assayed on rat brain membrane instead of guinea pig brain membrane. The pyridomorphinan and NTI analogues are opioid antagonists selective for the δ receptor, whereas cyprodime and phenylmorphan analogues are antagonists selective respectively for μ and κ receptors. Notwithstanding these variations, all compounds were well predicted by the present CoMFA models in terms of binding affinity (pK_i) for the three opioid receptors. The results are shown in Table 2 and plotted in Figure 2A−C. The average residuals for δ, μ, and κ receptor binding affinities are 0.45, 0.53, and 0.54 log units, respectively. Furthermore, these compounds all fit well within the regression trend line established by the training sets of the CoMFA models. The predicted κ binding affinities of compounds **83**−**96** are very close to their experimental values, despite the implicit uncertainties of cross-species extrapolation. It seems plausible that these compounds bind to both rat and guinea pig brain κ membranes in a similar fashion. In view of their excellent predictability across a broad range of structurally diverse opioid ligands that vary widely in affinity and selectivity for the opioid receptors, these CoMFA models provide valuable tools for guiding the rational design of novel opioids and for predicting their biological activity prior to chemical synthesis and biological testing.

Interpretation of CoMFA Models. The steric and electrostatic CoMFA color-contour maps can be regarded as visual representations of the 3D-QSAR models (Figure 3). The colored polyhedra represent spatial regions around the ligands where variations in steric or electrostatic fields are associated with differences in the target property (i.e., pK_i). The green (yellow) contours correspond to regions where increased steric bulk is favored (disfavored); the blue (red) contours correspond to regions where increased electropositive (electronegative) character is associated with enhanced ligand binding affinity. The individual contributions from the steric and electrostatic fields for the present models are 75%/25%, 65%/35%, and 67%/33%, respectively, for the δ, μ, and κ CoMFA models (Table 4). Such field contributions demonstrate that the variations in binding affinity among these antagonists are dominated by steric interactions with the three opioid receptor binding sites.

As our ultimate goal is to design δ selective ligands, the compounds selected for model development all exhibit binding affinity for the δ opioid receptor. Whereas the entire data set of 74 NTI analogues exhibit detectable δ binding affinity, some compounds with sterically bulky (e.g. Ph, compound **30**; 3-OH-Ph, compound **31**) and electronegative (e.g. methoxy, compounds **32**−**34**) substituents at position 3 (Table 1) are effectively devoid of binding affinity for the μ and κ opioid receptors. Hence, the corresponding μ and κ CoMFA models were constructed from biological data for 58 (59) compounds.

The interaction between opioid receptors and their ligands has been described in terms of the familiar "message−address" concept.[25,26] The "message" represents those structural features common to all opioids that are recognized similarly by the three types of receptors (δ, κ, and μ). The "address" represents those specific structural features that confer high selectivity for a particular opioid receptor subtype (e.g., δ). For ligands with morphine-like structure that are selective for the δ opioid receptor (i.e., NTI), the tyramine moiety corresponds to the "message" while the conformationally constrained steric groups linked to the morphinan nucleus (i.e., benzene on NTI) act as the "address" (Figure 1). This concept has been applied frequently in the past to design potent, subtype-selective opioid receptor ligands such as SIOM[27] and norNBI.[28]

CoMFA Contour Maps Are Consistent with the "Message" Concept. By comparing the steric and electrostatic maps for the three opioid receptor subtypes, common features were found in the tyramine moiety ("message") of all ligands. A large green polyhedron is located at the site of the substitutions on the basic nitrogen (N17) on all three steric maps, consistent with the observation that bulky N-substitutions on N17 of opioid antagonists are well-tolerated for the three receptor subtypes.[11,22] Yellow and blue polyhedra are present near the 3 position of NTI for the δ and κ receptors but not for the μ receptor (Figure 3), consistent with the complete loss of binding affinity for the μ receptor when sterically bulky (e.g. 2-furanyl, compound **29**) and electronegative (e.g. methoxy, compound **70**) substitutions occupy this position. This finding suggests that alkylation of phenolic hydroxyl and lipophilic substitutions at the 3 position are detrimental for binding to the three opioid receptors, which is in good agreement with the experimental SARs[8,22,29] and pharmacophore models of morphine-like opioids.[30]

CoMFA Contour Maps Are Consistent with the "Address" Concept. The most distinct color changes are found in regions around the indolic ring of NTI, corresponding to the "address" portion of δ receptor selective ligands (Figure 3). The CoMFA contour maps for the δ receptor model display a large green polyhedron nearby the δ "address" region; thus, sterically bulky substitutions at positions 5′, 6′, and 7′ (Table 1) are well tolerated for δ receptor binding (e.g., 5′-benzyloxy, compound **18**; 6′-phenoxy, compound **20**; and 7′-phenyl, compound **22**). In contrast, yellow polyhedra dominate this area on the maps for the μ and κ models, as evidenced by diminished binding affinity for the μ and κ receptors by 5′ substitutions, although 7′ substitutions are well-tolerated (e.g., 5′-phenyl, compound **16**). The absence of polyhedra (blue, red) around positions 4′, 5′, 6′, and 7′ of NTI on the δ electrostatic maps indicates that electrostatic effects on δ receptor binding are negligible in this region, which is consistent with the observation that halogen substitutions at these positions are well-tolerated for δ receptor binding.[29] In sharp contrast, the blue polyhedra located around positions 5′ on the μ maps and 1′, 2′, 5′, and 7′ on the κ maps are indicative that more electropositive groups are desirable for ligand binding to the μ and κ receptors. The large blue volume around the indolic ring on the κ electrostatic contour map coincides with the observation

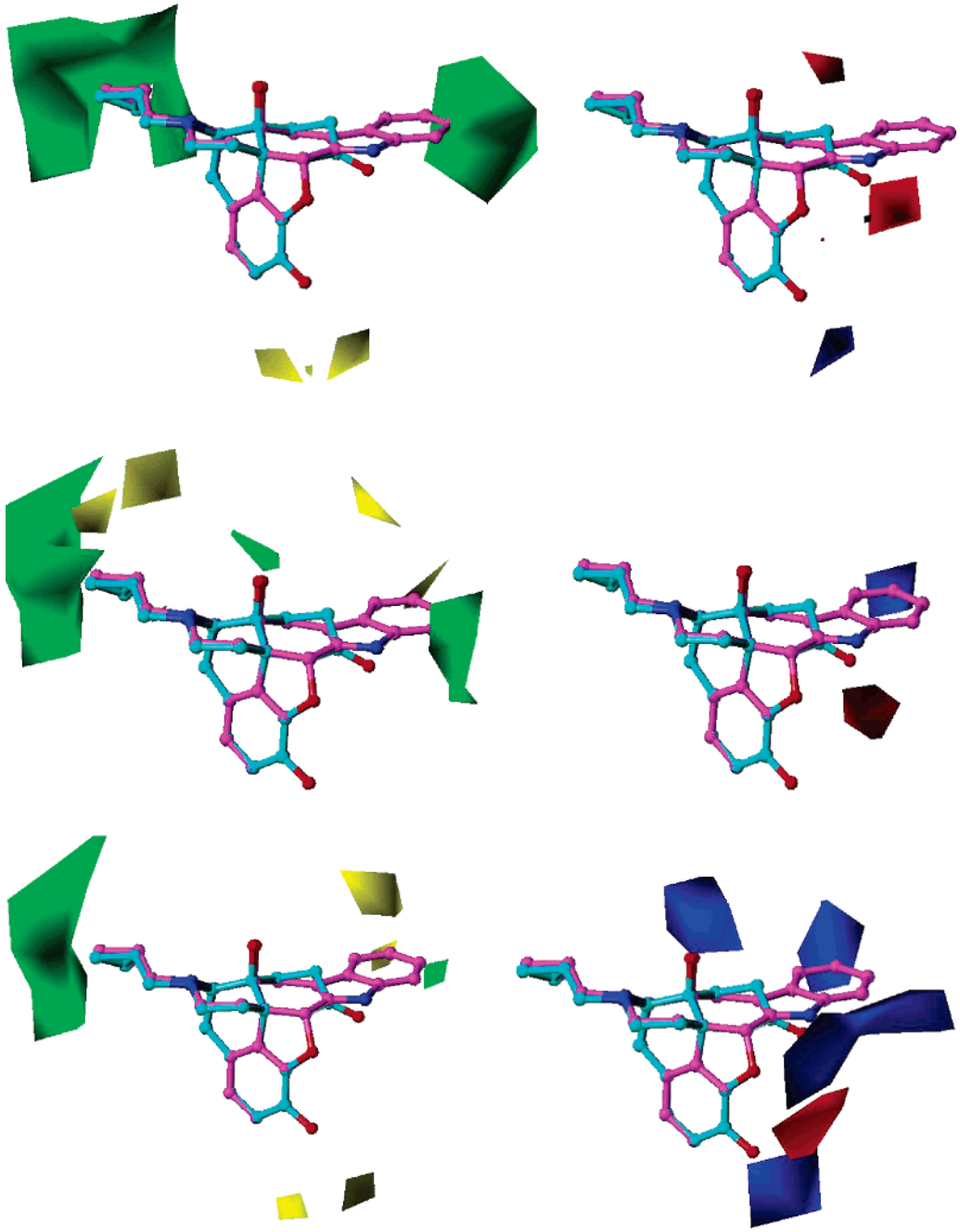

Figure 3. CoMFA steric (left) and electrostatic (right) contour maps for the δ (upper), μ (middle), and κ (lower) opioid receptors. To assist visual clarity, NTI and naltrexone are inserted into the maps as a ball-and-stick rendering with color-coded atom types: C (magenta and cyan), N (blue), and O (red). Regions around the ligands where sterically bulky groups are favorable (green) or unfavorable (yellow) for enhanced binding affinity are color-coded accordingly. Similarly, regions where electronegative (blue) and electropositive (red) groups are favorable for enhanced ligand binding are colored accordingly.

that a secondary basic group (e.g., 5′-*E*-CH=CH-pyridinyl, compound **25**) acts as the κ receptor "address" in this region.[31−34] Furthermore, the red polyhedron near the 5 position of naltrexone on the δ and μ maps suggests that electronegative substitutions at this position are favorable for the binding of naltrexone analogues to the δ and μ receptors. This interpretation is consistent with the finding that the presence of pyridine (e.g., compound **47**) and carbonyl (e.g., compound **4**) at this position is favorable for δ and μ receptor binding, respectively. In contrast, the blue polyhedron located in this region on the κ maps indicates that electropositive substitutions (e.g. NH, compound **69**) are favorable for κ receptor binding.

Additional Implications Suggested by the CoMFA Contour Maps. In addition to similarities in the "message" region and differences in the "address" region, distinctions are also observed around positions 8 and 14 of NTI (Table 1). The substitutions in this region (e.g., 14-H and 8-Me, compound **36**) have negligible effects on the binding affinities for the δ opioid receptor; therefore, colored polyhedra are absent here. This result concurs with findings that the replacement of 14-hydroxyl by hydrogen and the alkylation of 14-aminomorphinedole produced little effect on δ binding affinity.[22,35] The green polyhedron on the μ maps suggests that sterically bulky substitutions (e.g., 8-Me, compound **38**) are desirable for increasing binding affinity for the

μ opioid receptor, while the blue polyhedron on the κ maps suggests that electropositive substitutions (e.g., 14-OH, compound **46**) in this region are favorable for binding to the κ opioid receptor. The SARs derived from interpretation of this region should provide additional clues for conferring subtype selectivity in addition to the "address" moiety.

Comparison of the CoMFA maps indicates that the presence of a bulky moiety in the "address" region is crucial for δ selectivity, while a second basic group confers selectivity for κ opioid receptor. This conclusion essentially reiterates a key tenet of the "message−address" concept, specifically, that selectivity of NTI and its analogues for the δ opioid receptor is attributed to the presence of a bulky group attached to the morphinan nucleus[9,17] and that selectivity for the κ opioid receptor results from the existence of a second basic group.[31−34]

Our laboratory is particularly interested in delineating the pharmacophoric elements for conferring high binding affinity and selectivity for the δ opioid receptor. To achieve high selectivity for δ over μ and κ opioid receptors, approaches are suggested by the present CoMFA models to enhance the binding affinity for δ receptor or to decrease the binding affinity for μ and κ receptors. For example, introduction of bulky groups at the 5′ position of NTI is predicted to enhance δ selectivity by increasing the δ binding affinity while decreasing the μ and κ binding affinity. Electronegative substitutions at the 5′ position are predicted to decrease the binding affinity for the μ and κ receptors but have little effect on δ binding affinity, with a net effect of enhancing selectivity for the δ receptor. In addition, structural modification at positions 8 and 14 of NTI could also confer δ selectivity. Less bulky substitutions at position 8 are predicted to be less favorable for μ compared with δ receptor binding. Likewise, electronegative substitutions at position 14 are predicted less favorable for κ compared with δ binding, leading to enhanced selectivity for the δ receptor.

Summary and Conclusions

3D-QSAR models were constructed in order to gain insights into the SARs of opioid receptor antagonists. A large data set for opioid antagonists with classic opiate structures was created by pooling ligand information from different studies to obtain significant and useful CoMFA models. A process of "leave one data set out", similar to traditional "leave one out" cross-validation procedure employed in partial least-squares (PLS) analysis, was utilized to study the feasibility of pooling data from different sources. These studies demonstrated the feasibility of this approach for the present application. Separate CoMFA models were developed from the pooled data set for the δ, μ, and κ antagonists. These CoMFA models showed excellent internal predictability and consistency, and validation using test-set compounds yielded a predicted pK_i value within 1 log unit of the experimental value in all cases. The predictive ability of the present models is further substantiated by the predictive r^2: 0.70 (δ), 0.89 (μ), and 0.77 (κ). An external test set consisting of five distinct, structurally diverse, core structures was selected to further evaluate the predictability of the CoMFA models. Consistently good predictions for the external test-set compounds substantiate the robust predictive power of these CoMFA models, thus recommending their utility in predicting the binding affinities for compounds beyond those considered in the present study.

CoMFA field analysis demonstrated that variations in the binding affinity of opioid antagonists are dominated by steric rather than electrostatic interactions with the three opioid receptor subtypes. By comparing the steric and electrostatic contour maps among the three opioid receptors, common patterns were found with respect to substitutions at O3 and N17 corresponding to the "message" region of opioid receptor ligands. As would be expected, significant differences in the CoMFA contour maps were observed in the "address" region. Differences were also found in the region of positions 8 and 14 of NTI. Bulky and electronegative substitutions at position 5′ of NTI are predicted to increase the selectivity for δ over μ and κ opioid receptors. Likewise, less bulky substitutions at position 8 and electronegative substitutions at position 14 are predicted to enhance selectivity for the δ receptor. These SAR observations, together with the CoMFA models, may find use in the rational design of novel opioid antagonists and in the prediction of their relative binding affinity for the δ, μ, and κ opioid receptors.

Acknowledgment. Funding for this research was provided by the Biotechnology Research & Development Corp. (BRDC, Peoria, IL), by a High-Technology Workforce Excellence Grant from the New Jersey Commission on High Education, and by the Informatics Institute of the University of Medicine and Dentistry of New Jersey (http://informatics.umdnj.edu/).

References

(1) Dhawan, B. N.; Cesselin, F.; Raghubir, R.; Reisine, T.; Bradley, P. B.; Portoghese, P. S.; Hamon, M. International Union of Pharmacology. XII. Classification of opioid receptors. *Pharmacol. Rev.* **1996**, *48*, 567−592.

(2) Pert, C. B.; Snyder, S. H. Opiate receptor: Demonstration in nervous tissue. *Science* **1973**, *179*, 1011−1014.

(3) Law, P. Y.; Wong, Y. H.; Loh, H. H. Molecular mechanisms and regulation of opioid receptor signaling. *Annu. Rev. Pharmacol. Toxicol.* **2000**, *40*, 389−430.

(4) Abdelhamid, E. E.; Sultana, M.; Portoghese, P. S.; Takemori, A. E. Selective blockage of delta opioid receptors prevents the development of morphine tolerance and dependence in mice. *J. Pharmacol. Exp. Ther.* **1991**, *258*, 299−303.

(5) Reid, L. D.; Hubbell, C. L.; Glaccum, M. B.; Bilsky, E. J.; Portoghese, P. S.; Porreca, F. Naltrindole, an opioid delta receptor antagonist, blocks cocaine-induced facilitation of responding for rewarding brain stimulation. *Life Sci.* **1993**, *52*, PL67−71.

(6) House, R. V.; Thomas, P. T.; Kozak, J. T.; Bhargava, H. N. Suppression of immune function by nonpeptidic delta opioid receptor antagonists. *Neurosci. Lett.* **1995**, *198*, 119−122.

(7) Schiller, P. W.; Fundytus, M. E.; Merovitz, L.; Weltrowska, G.; Nguyen, T. M.; Lemieux, C.; Chung, N. N.; Coderre, T. J. The opioid mu agonist/delta antagonist DIPP−NH(2)[Psi] produces a potent analgesic effect, no physical dependence, and less tolerance than morphine in rats. *J. Med. Chem.* **1999**, *42*, 3520−3526.

(8) Coop, A.; Rothman, R. B.; Dersch, C.; Partilla, J.; Porreca, F.; Davis, P.; Jacobson, A. E.; Rice, K. C. Delta opioid affinity and selectivity of 4-hydroxy-3-methoxyindolomorphinan analogues related to naltrindole. *J. Med. Chem.* **1999**, *42*, 1673−1679.

(9) Portoghese, P. S. Edward E. Smissman-Bristol-Myers Squibb Award Address. The role of concepts in structure−activity relationship studies of opioid ligands. *J. Med. Chem.* **1992**, *35*, 1927−1937.

(10) Portoghese, P. S.; Sultana, M.; Takemori, A. E. Naltrindole, a highly selective and potent non-peptide delta opioid receptor antagonist. *Eur. J. Pharmacol.* **1988**, *146*, 185−186.

(11) McLamore, S.; Ullrich, T.; Rothman, R. B.; Xu, H.; Dersch, C.; Coop, A.; Davis, P.; Porreca, F.; Jacobson, A. E.; Rice, K. C. Effect of N-alkyl and N-alkenyl substituents in noroxymorphindole, 17-substituted-6,7-dehydro-4,5α-epoxy-3,14-dihydroxy-6,7:2′,3′-indolomorphinans, on opioid receptor affinity, selectivity, and efficacy. *J. Med. Chem.* **2001**, *44*, 1471−1474.
(12) Ananthan, S.; Johnson, C. A.; Carter, R. L.; Clayton, S. D.; Rice, K. C.; Xu, H.; Davis, P.; Porreca, F.; Rothman, R. B. Synthesis, opioid receptor binding, and bioassay of naltrindole analogues substituted in the indolic benzene moiety. *J. Med. Chem.* **1998**, *41*, 2872−2881.
(13) Ananthan, S.; Kezar, H. S., 3rd; Carter, R. L.; Saini, S. K.; Rice, K. C.; Wells, J. L.; Davis, P.; Xu, H.; Dersch, C. M.; Bilsky, E. J.; Porreca, F.; Rothman, R. B. Synthesis, opioid receptor binding, and biological activities of naltrexone-derived pyrido- and pyrimidomorphinans. *J. Med. Chem.* **1999**, *42*, 3527−3538.
(14) Yu, H.; Prisinzano, T.; Dersch, C. M.; Marcus, J.; Rothman, R. B.; Jacobson, A. E.; Rice, K. C. Synthesis and biological activity of 8β-substituted hydrocodone indole and hydromorphone indole derivatives. *Bioorg. Med. Chem. Lett.* **2002**, *12*, 165−168.
(15) Ullrich, T.; Dersch, C. M.; Rothman, R. B.; Jacobson, A. E.; Rice, K. C. Derivatives of 17-(2-methylallyl)-substituted noroxymorphone: Variation of the delta address and its effects on affinity and selectivity for the delta opioid receptor. *Bioorg. Med. Chem. Lett.* **2001**, *11*, 2883−2885.
(16) Kubota, H.; Rothman, R. B.; Dersch, C.; McCullough, K.; Pinto, J.; Rice, K. C. Synthesis and biological activity of 3-substituted 3-desoxynaltrindole derivatives. *Bioorg. Med. Chem. Lett.* **1998**, *8*, 799−804.
(17) Kshirsagar, T. A.; Fang, X.; Portoghese, P. S. 14-Desoxy analogues of naltrindole and 7-spiroindanyloxymorphone: The role of the 14-hydroxy group at delta opioid receptors. *J. Med. Chem.* **1998**, *41*, 2657−2660.
(18) Gao, P.; Larson, D. L.; Portoghese, P. S. Synthesis of 7-arylmorphinans. Probing the "address" requirements for selectivity at opioid delta receptors. *J. Med. Chem.* **1998**, *41*, 3091−3098.
(19) Le Dain, A. C.; Madsen, B. W.; Skelton, B. W.; White, A. H. Crystal structure of naltrexone hydrocholide: Implications for location of the nicotinic receptor noncompetitive inhibor binding site. *Aust. J. Chem.* **1992**, *45*, 635−640.
(20) *Sybyl 6.8*; Tripos, Inc.: St. Louis, MO.
(21) Thomas, J. B.; Atkinson, R. N.; Namdev, N.; Rothman, R. B.; Gigstad, K. M.; Fix, S. E.; Mascarella, S. W.; Burgess, J. P.; Vinson, N. A.; Xu, H.; Dersch, C. M.; Cantrell, B. E.; Zimmerman, D. M.; Carroll, F. I. Discovery of an opioid kappa receptor selective pure antagonist from a library of N-substituted 4β-methyl-5-(3-hydroxyphenyl)morphans. *J. Med. Chem.* **2002**, *45*, 3524−3530.
(22) Ananthan, S.; Khare, N. K.; Saini, S. K.; Seitz, L. E.; Bartlett, J. L.; Davis, P.; Dersch, C. M.; Porreca, F.; Rothman, R. B.; Bilsky, E. J. Identification of opioid ligands possessing mixed micro agonist/delta antagonist activity among pyridomorphinans derived from naloxone, oxymorphone, and hydromorphone. *J. Med. Chem.* **2004**, *47*, 1400−1412.
(23) Spetea, M.; Schullner, F.; Moisa, R. C.; Berzetei-Gurske, I. P.; Schraml, B.; Dorfler, C.; Aceto, M. D.; Harris, L. S.; Coop, A.; Schmidhammer, H. Synthesis and biological evaluation of 14-alkoxymorphinans. 21. Novel 4-alkoxy and 14-phenylpropoxy derivatives of the mu opioid receptor antagonist cyprodime. *J. Med. Chem.* **2004**, *47*, 3242−3247.
(24) Schmidhammer, H.; Daurer, D.; Wieser, M. Synthesis and biological evaluation of 14-alkoxymorphinans.14. 14-ethoxy-5-methyl substituted indolomorphinans with delta opioid receptor selectivity. *Bioorg. Med. Chem. Lett.* **1997**, *7*, 151−156.
(25) Schwyzer, R. ACTH: A short introductory review. *Ann. N.Y. Acad. Sci.* **1977**, *297*, 3−26.
(26) Portoghese, P. S. Bivalent ligands and the message-address concept in the design of selective opioid receptor antagonists. *Trends Pharmacol. Sci.* **1989**, *10*, 230−235.
(27) Portoghese, P. S.; Moe, S. T.; Takemori, A. E. A selective delta 1 opioid receptor agonist derived from oxymorphone. Evidence for separate recognition sites for delta 1 opioid receptor agonists and antagonists. *J. Med. Chem.* **1993**, *36*, 2572−2574.
(28) Takemori, A. E.; Portoghese, P. S. Selective naltrexone-derived opioid receptor antagonists. *Annu. Rev. Pharmacol. Toxicol.* **1992**, *32*, 239−269.
(29) Portoghese, P. S.; Sultana, M.; Takemori, A. E. Design of peptidomimetic delta opioid receptor antagonists using the message-address concept. *J. Med. Chem.* **1990**, *33*, 1714−1720.
(30) Shenderovich, M. D.; Liao, S.; Qian, X.; Hruby, V. J. A three-dimensional model of the delta-opioid pharmacophore: Comparative molecular modeling of peptide and nonpeptide ligands. *Biopolymers* **2000**, *53*, 565−580.
(31) Portoghese, P. S.; Nagase, H.; Takemori, A. E. Only one pharmacophore is required for the kappa opioid antagonist selectivity of norbinaltorphimine. *J. Med. Chem.* **1988**, *31*, 1344−1347.
(32) Lin, C. E.; Takemori, A. E.; Portoghese, P. S. Synthesis and kappa-opioid antagonist selectivity of a norbinaltorphimine congener. Identification of the address moiety required for kappa-antagonist activity. *J. Med. Chem.* **1993**, *36*, 2412−2415.
(33) Stevens, W. C., Jr.; Jones, R. M.; Subramanian, G.; Metzger, T. G.; Ferguson, D. M.; Portoghese, P. S. Potent and selective indolomorphinan antagonists of the kappa-opioid receptor. *J. Med. Chem.* **2000**, *43*, 2759−2769.
(34) Metzger, T. G.; Paterlini, M. G.; Ferguson, D. M.; Portoghese, P. S. Investigation of the selectivity of oxymorphone- and naltrexone-derived ligands via site-directed mutagenesis of opioid receptors: Exploring the "address" recognition locus. *J. Med. Chem.* **2001**, *44*, 857−862.
(35) Grundt, P.; Jales, A. R.; Traynor, J. R.; Lewis, J. W.; Husbands, S. M. 14-amino, 14-alkylamino, and 14-acylamino analogues of oxymorphindole. Differential effects on opioid receptor binding and functional profiles. *J. Med. Chem.* **2003**, *46*, 1563−1566.
(36) Harnett, D. L.; Murphy, J. L. *Introductory Statistical Analysis*; Addison-Wesley Publishing Co.: Philippines, 1975; p 430.

JM049117E